Femtosecond Time-Resolved Pump−Probe Spectroscopy of NaI in Rare-Gas Environment†

G. Knopp, M. Schmitt, A. Materny, and W. Kiefer*

Institut für Physikalische Chemie der Universität Würzburg, Am Hubland, D-97074 Würzburg, Federal Republic of Germany

Received: February 20, 1997; In Final Form: April 8, 1997⊗

In this paper we report femtosecond studies of the influence of rare-gas collisions on the dissociation reaction of NaI molecules by investigating the coherent wave packet motion in NaI at a temperature of 670 °C and rare-gas pressures ranging from 0 to 1000 bar. The photodissociation dynamics of NaI is influenced by the interaction between the excited covalent and the ionic ground state potential energy surfaces, which cross at a certain internuclear separation. Due to the adiabaticity of the so formed potential, studies of the elementary nuclear motion and reaction dynamics along the covalent (Na + I) and the ionic ($Na^+ + I^-$) channels are possible. The probing is made for the transition-state complex $[Na\cdots I]^{\ddagger}$*. Even at low rare-gas pressures a considerable influence of collisions on the wave packet motion within the adiabatic potential well is found. Only few collisions between NaI molecules and surrounding rare-gas atoms result in fast vibrational relaxation and loss of coherence. Furthermore, a stabilization of the transition state is observed due to the decrease of the Landau−Zener escape probability. The reaction cross section for the interaction of the transition state molecules with helium atoms is found to be smaller than for the interaction with argon atoms. The intensity of the detected laser-induced fluorescence arising from the transition Na ← Na* decreases with increasing rare-gas pressure. Here, the effect for argon atoms is smaller than for helium atoms.

1. Introduction

Electronic curve-crossing processes in solution are an important aspect of condensed phase chemical reaction dynamics.[1,2] The interaction of reacting molecules with their solvents induces changes in the potential energy surfaces as well as reaction trajectories. The photodissociation of iodine served as a prototype reaction for the investigation of solute−solvent interactions since the early work of Franck and Rabinowitch.[3,4] Their main interest was focused on the *cage effect*, which results in a geminate recombination of the fragments. First experimental investigations by Zimmerman and Noyes[5] triggered theoretical and experimental studies in many research groups (for a review see ref 6).

First investigations of the fast reaction dynamics disturbed by solute−solvent interaction were performed by Chuang *et al.*[7] In this work picosecond time-resolved studies on iodine in CCl_4 and hexadecane were presented. From their transients they found two time scales of ≈10 and ≈100 ps, which they related to predissociation and caging, respectively. Nesbitt and Hynes[8] as well as Wilson and co-workers[9] showed that the dynamics on the time scale of ≈100 ps is due to relatively slow vibrational relaxation within the electronic ground X state. In their experiments, Kelley *et al.*[10] were able to demonstrate that also the excited A and A′ states play an important role in the recombination reaction. A more detailed picture of the involved reaction dynamics could be given by Harris and co-workers.[11,12] Predissociation processes faster than 2 ps had to be assumed to explain their findings.

Therefore, in order to gain a microscopic picture of the dissociation and recombination dynamics of iodine, spectroscopy on a femtosecond time scale had to be applied. The pioneering work of Zewail and co-workers demonstrated the femtosecond dynamics of I_2 in a gas cell and in a molecular beam.[13,14] Also, the dynamics of the isolated molecules have been contrasted with those of high-pressure gases[15,16] and in clusters with rare-gas atoms.[17,18] In a series of papers (*Solvation Ultrafast Dynamics of Reactions*, see articles in ref 19), they elucidate the real-time elementary dynamics of reactions in solutions. Very recently, three papers in this series reported studies of femtosecond dynamics of dissociation and recombination processes of I_2 in supercritical rare-gas solvents.[20−22] By changing the solvent pressure from 0 to about 3000 bar, the effect of solvation on reaction dynamics could be studied in a systematic way from ideal gas to liquidlike fluid conditions. The results give interesting details of the changes of the reaction trajectories that can be compared to results obtained from femtosecond experiments in solution by Scherer *et al.*,[23] in rare-gas clusters by Zewail's group,[24] and in argon matrices by Apkarian and co-workers.[25,26]

In this paper we present results of femtosecond experiments performed on NaI molecules in supercritical rare-gas solvents. The dissociation of NaI in real time has been studied extensively, both experimentally and theoretically.[27−32] In contrast to purely dissociative reactions, the reaction of NaI

$$NaI^* \rightarrow [Na\cdots I]^{\ddagger *} \rightarrow \begin{cases} Na(^2S_{1/2}) + I(^3P_{3/2}) & (\text{for } \Omega = 0^+, 1) \\ Na^+(^1S_0) + I^-(^1S_0) & (\text{for } \Omega = 0^+) \end{cases} \quad (1)$$

is affected by a non-Born−Oppenheimer coupling of the ionic ground state $[X(^1\Sigma^+)]$ and the lowest excited covalent state $[A(0^+)$, Hund's case c coupling]. Due to this avoided crossing, the $A(0^+)$ covalent state and the ionic ground state interact at their crossing point R_x (≈6.9 Å). The femtosecond experiments have explored the resonant wave packet motion of the $[Na\cdots I]^{\ddagger}$* transition state.[27−31] In Figure 1 the experimental scheme and the involved potential curves[31,33] are shown. A femtosecond pump pulse prepares the system on the repulsive branch of the repulsive $A(0^+)$ state. The subsequent nuclear motion is probed by absorption $[C(0^+) \leftarrow A(0^+)]$ of a second femtosecond pulse,

† This paper is dedicated to Professor Ahmed H. Zewail on the occasion of his 50th birthday.

* Author to whom correspondence should be addressed.

⊗ Abstract published in *Advance ACS Abstracts,* June 15, 1997.

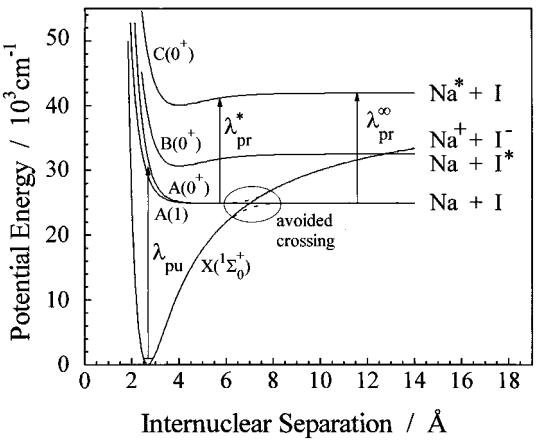

Figure 1. Relevant potential energy curves for the dissociation reaction on NaI. The labels at right correspond to the diabatic potential curves. The pump pulse λ_{pu} prepares the system on the excited A(0^+) surface. The probe pulse monitors either the transition-state region (λ^*_{pr}) or the produced Na atoms (λ^∞_{pr}).

delayed in time relatively to the first. The wavelength of the second pulse determines at what reaction coordinate the dynamics are probed.[34,35] *On-resonance* probing (λ^∞_{pr} in Figure 1) is resonant with the Na D-line transitions and, therefore, yields the stepwise buildup of free Na atoms. If the probe is tuned away from the atomic resonance, the resulting transient corresponds to the dynamics of the wave packet oscillating inside the adiabatic well (*off-resonance* probing, λ^*_{pr} in Figure 1). Due to the nonadiabatic curve crossing, the wave packet leaks through the Landau−Zener[36] coupled region with a certain escape probability (≈10% for $\lambda_{pu} = 310$ nm). This results in a vanishing λ^*_{pr} signal intensity for longer delay times (≥40 ps for $\lambda_{pu} = 310$ nm).

In the following (section 2), a brief description of the experimental setup is provided for both the high-temperature/high-pressure apparatus and the femtosecond laser system. In section 3, we present experimental results obtained from pump−probe experiments on NaI molecules in rare-gas solvents at different pressures. Emphasis is put on the role of the avoided crossing. Experimental problems are discussed as well. Finally, concluding remarks are given in section 4.

2. Experimental Section

The experiments described in this paper were performed using two ultrashort laser pulses centered at 320 and 620 nm for pumping and probing, respectively. The pulses were about 70 fs long and had energies between 0.5 and 1 μJ. The setup used for the pump-probe experiment is shown in Figure 2.

The laser system is based on a Ti:Sapphire oscillator (Coherent MIRA) pumped by the multiline output of an Ar^+ ion laser (Coherent Innova 310) running at about 8 W. The pulses were produced by the oscillator at a repetition rate of 76 MHz having temporal pulse widths of about 100 fs. The pulse energy was less than 10 nJ, and the pulses were centered at about 800 nm having a spectral width (fwhm) of 14 nm. For the amplification of the pulses a regenerative Ti:sapphire amplifier system (Clark-MXR) was used. The pulses were stretched to a duration of >200 ps before amplification. The regenerative Ti:sapphire amplifier was pumped by a frequency-doubled Nd:YAG laser at a repetition rate of 1 kHz. After recompression the pulses had energies of ≈1.5 mJ and temporal widths of less than 100 fs.

In order to have two different colors available, the 800 nm pulse train was split into two parts by means of a beam splitter. Using two four-path OPGs (optical parametric generators, Light Conversion), two independent wavelengths could be chosen. The laser pulses in the visible spectral range were produced using sum frequency generation between signal and idler output of the OPG as well as second harmonic generation of either the signal or the idler light. The pulses were finally compressed in double-pass two-prism arrangements resulting in temporal pulse widths of about 70 fs (assuming Gaussian pulse profiles). The 320 nm pump pulse was generated by frequency doubling in a thin, phase-matched BBO crystal. The spectral widths of the pulses were about 10 nm for both pump and probe laser.

The pump and the probe pulses were delayed in time relative to one another in a Michelson interferometer arrangement. The beams were collinearly recombined by means of a dielectric beam splitter and were focused into the high-pressure cell. Laser-induced fluorescence (LIF) was collected orthogonal to the coincident laser beams. After suppressing unshifted stray light of the lasers by means of a computer-controlled 50 cm monochromator (Acton SpectraPro-500), the signal was detected with a fast photomultiplier tube (RCA C31024 A) as a function of delay time. The signal-to-noise ratio was enhanced by use of a boxcar integrator (EG&G model 4121B) in gated-integrator mode, as well as by numerical averaging of several pulses. The relative timing between the two pulses was varied with a computer-controlled actuator that allowed for optical delays up to 3 ns with a minimal step size of 6 fs. Two hundred data points were accumulated at each actuator position.

The sample (NaI) was put into a high-pressure cell specially designed for these experiments (see Figure 3). The high-pressure cell was built from a heat-treated nickel−cobalt alloy (RGT 601) with a tensile strength of about 1000 N/mm^2 up to temperatures of ≈700 °C. Four optical sapphire windows (∅ 10 mm, free aperture 6 mm, thickness 6 mm) allowed for two optical transmission axes being orthogonal to each other. In order to allow high pressures at high temperatures, special gold seals had to be used for the windows. The total cell volume was about 1 cm^3. Such a small cell volume was essential in order to reach high pressures (up to 3.5 kbar) using manually operated, screw-type pressure generators. The starting pressure (≈300 bar) was supplied by a pressure pump (Hofer model 52HK25). Pressure inside the cell was monitored using a precision strain gauge pressure transducer. The cell showed no change in gas pressure during the course of an experiment. The pressure chamber was placed in an oven. During the experiments the temperature was maintained at approximately 670 °C. The vapor pressure of the sample was estimated to be about 100−200 mTorr, corresponding to a number density of (5−10) × 10^{17} molecules/cm^3 for the NaI.[37]

3. Results and Discussion

In this section, we present the results obtained from a series of experiments in compressed supercritical argon or helium gas at a temperature of 670 °C and pressure ranging from 0 to 1000 bar. Ground state NaI molecules were excited with pump pulses that were centered at 320 nm and had a temporal pulse width of about 70 fs. Absorption of the pump photon by the molecules is associated with a vertical transition from the ionic to the covalent surfaces [A(0^+,1) ← X($^1\Sigma^+$)]. The width of the wave packet at $\Delta t = 0$ is determined by the temporal and spectral width of the optical pump pulse as well as the shape of the excited potential curve. Using pulses centered at 620 nm for probing gives the dynamics of the wave packet moving periodically within the adiabatic potential well formed by the interaction of ground X($^1\Sigma^+$) and excited A(0^+) states (*off-resonance* probing in Figure 1).[27−31] The probe laser is absorbed

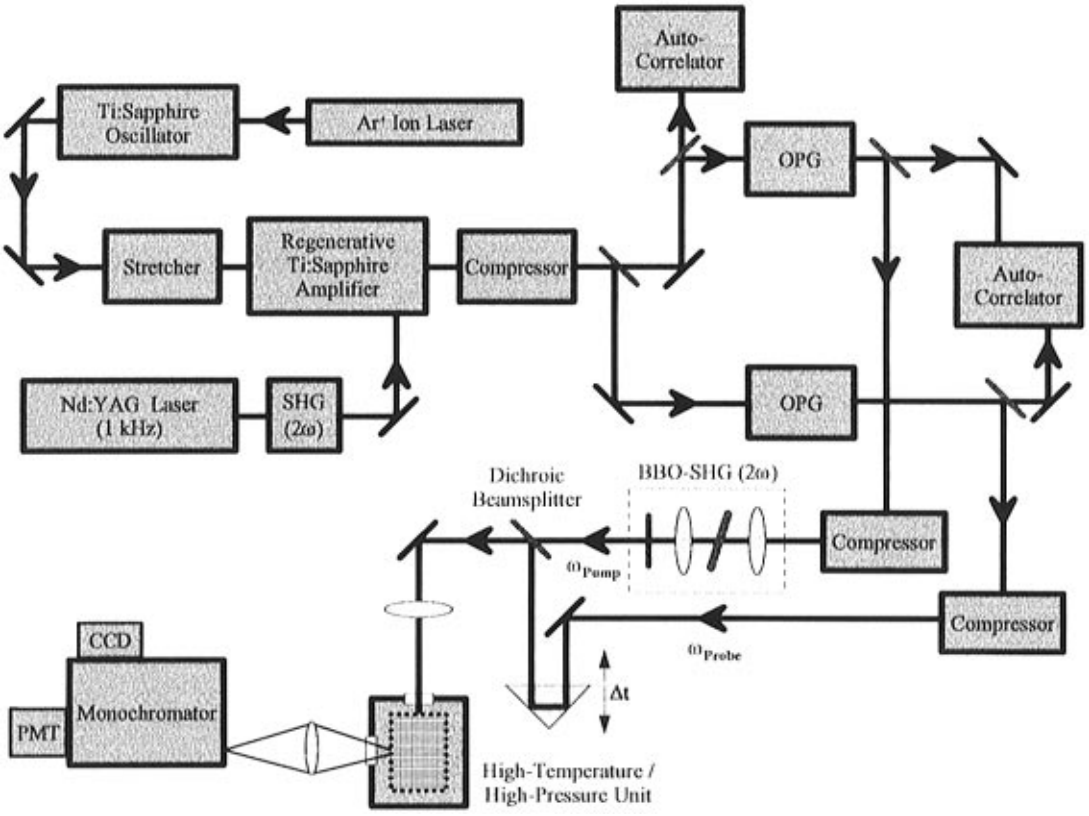

Figure 2. Schematic of the optical setup used in our experiments. For further details, see text.

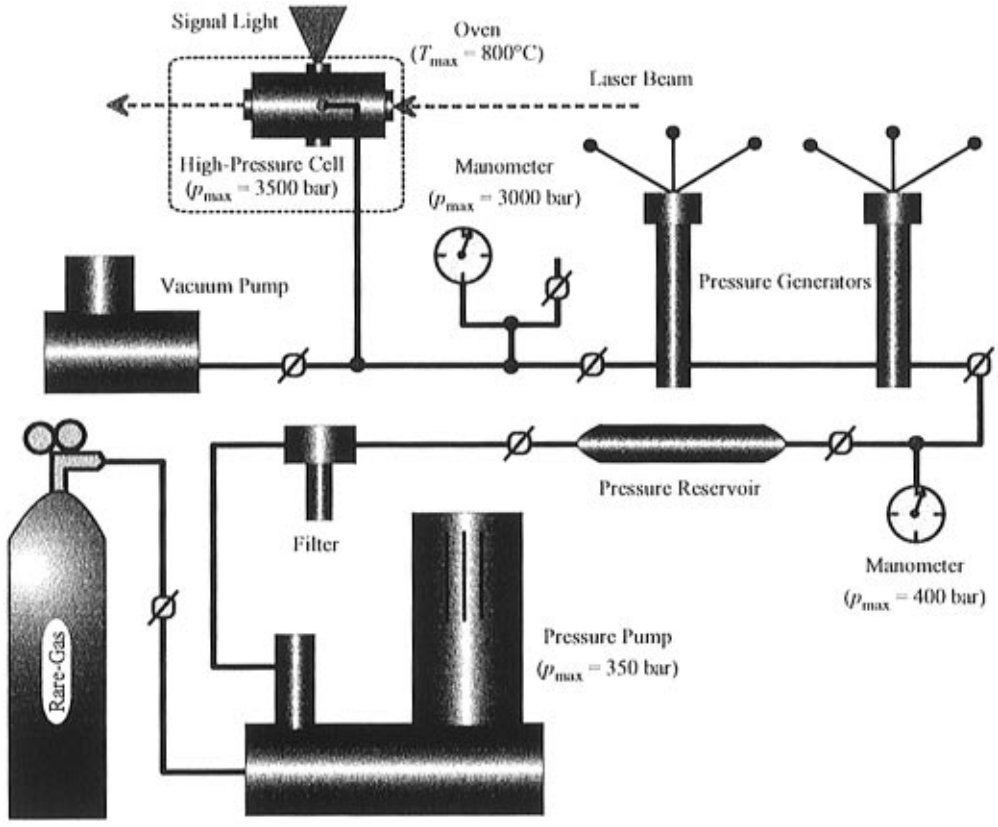

Figure 3. Schematic of the high-pressure system. For further details, see text.

$[C(0^+) \leftarrow A(0^+)]$ by the $[Na\cdots I]^{\ddagger *}$ transition state molecules, which finally results in excited sodium atoms $[Na^*(^2P_{1/2,3/2})]$ giving rise to fluorescence. The fluorescence signal (Na D-line transitions at 589.0 and 589.6 nm) as a function of delay time between pump and probe pulse should for rare-gas pressures of 0 bar be comparable to transients found for free NaI molecules by Zewail and co-workers.[27,28]

In Figure 4, a pump−probe transient taken from free NaI (p = 0 bar) in the high-pressure cell is shown. The transient observed displays the oscillatory behavior of the wave packet

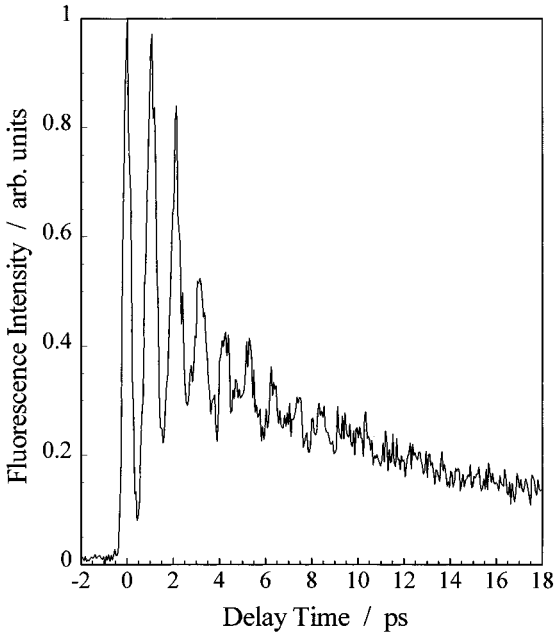

Figure 4. Pump−probe transient taken from free NaI (rare-gas pressure $p = 0$ bar) in the high-pressure cell. (Also valid for all other transients shown in this paper: The sample was heated to $T = 670$ °C in order to have sufficient vapor pressure. The probe wavelength was $\lambda_{pr}^{*} = 620$ nm monitoring the wave packet within the adiabatic $A(0^+)$ potential well.)

within the adiabatic potential well. The repetition rate of the observed signal maximum is the frequency of the wave packet in the potential well. The Fourier transform of the modulated transient shows frequency components which correspond to the energy differences $E(v_{i+1}) - E(v_i)$ between adjacent vibrational eigenstates of the adiabatic $A(0^+)$ state. For the pump wavelength chosen in our experiment ($\lambda_{pu} = 320$ nm), we determined a wavenumber difference of $\approx$27.5 cm^{-1}. This correlates to an oscillation time of $T \approx 1.2$ ps, which is in good agreement with the findings of Cong *et al.*[31]

The observed damping of the transient is due to three processes:[27,28] (i) The wave packet prepared on the A(1) excited state escapes within very short time as the potential curve is purely repulsive. A contribution to the light-induced fluorescence (LIF) signal therefore only can be seen at the position of the first maximum of the transient. (ii) The decay of the overall signal intensity reflects the population loss in the originally excited adiabatic $A(0^+)$ state, due to the predissociation, caused by the non-Born−Oppenheimer coupling of the $X(^1\Sigma_0^+)$ and the $A(0^+)$ state of the NaI molecule. The production of Na atoms can be detected by *on-resonance* probing (compare Figure 1). (iii) The even faster decreasing of the oscillation amplitudes is due to a dephasing of the wave packet.

The avoided crossing can be described using the Landau−Zener formalism:[29]

$$P_{LZ} = \exp\left[-\frac{4\pi^2}{h v_r(E, J)} \frac{V_{01}^2}{\frac{d}{dR}|V_{00} - V_{11}|}\right] \qquad (2)$$

Here, P_{LZ} describes the dissociation probability of the NaI molecule as a function of the relative velocity of the particles at the crossing point (for NaI at the internuclear distance $R \approx 6.9$ Å). V_{01} is the coupling energy between the two potential surfaces V_{00} and V_{11} at this point, which is about 370 cm^{-1} in our case.[29] The derivative gives the difference in slopes of the surfaces, and $v_r(E, J)$ is the recoil velocity which is a function

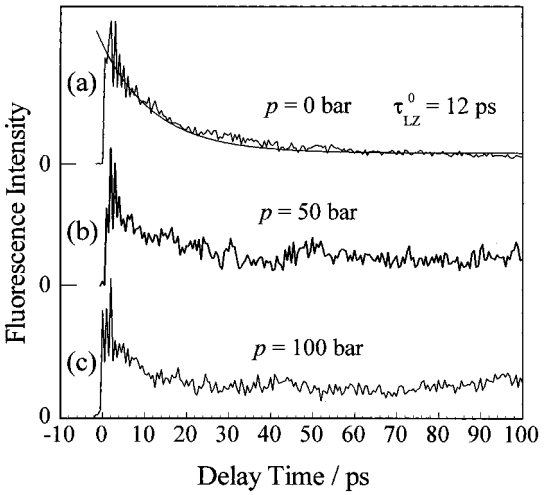

Figure 5. Pump−probe transients taken from NaI in the high-pressure cell for different helium gas pressures. (a) Unperturbed case $p = 0$ bar; fitting of the single exponential expression (eq 3) to the experimental data results in a Landau−Zener lifetime of $\tau_{LZ}^0 \approx 12$ ps. (b) $p = 50$ bar and (c) $p = 100$ bar; the decay behavior changes due to vibrational relaxation and can no longer be described by a single-exponential function. For details, see text.

of the total energy E as well as the rotational quantum number J. This predissociation results in a decay of the overall intensity of the detected fluorescence, which can be described using a single-exponential ansatz[21]

$$A(t) = A_0 \cdot \exp\left(-\frac{t}{\tau_{LZ}^0}\right) \qquad (3)$$

where τ_{LZ}^0 is a measure for the lifetime of the wave packet on the adiabatic potential surface. As a result of eq 2 this lifetime should increase with decreasing recoil velocity $v_r(E, J)$ or equivalent with decreasing total energy E.

By fitting the single-exponential expression (eq 3) to our experimental data, we obtained for the unperturbed case ($p = 0$ bar) $\tau_{LZ}^0 \approx 12$ ps (see Figure 5a). This corresponds to a Landau−Zener escape probability of $P_{LZ} \approx 0.10$, which is in a good agrement with the value determined by Rose *et al.*[29] ($P_{LZ} = 0.11$).

Going to higher rare-gas pressures ($p \geq 50$ bar), several changes could be observed: (i) The intensity of the LIF decreases with increasing rare-gas density. (ii) As the pressure becomes higher, the decay behavior of the overall signal intensity changes; a constant residual fluorescence signal can be observed for the whole accessible range of delay times. (iii) Coherence lifetimes decrease exponentially with increasing rare-gas pressure. These points are discussed in detail in the following.

(i) The decrease of the LIF signal with increasing rare gas density caused considerable experimental difficulties. Only transients up to a pressure of about $p = 1000$ bar could be obtained. Therefore, the signal-to-noise ratio decreased drastically for high-pressure transients. The reason for this effect can be easily understood if one considers the interaction of the rare-gas atoms with the excited $C(0^+)$ state as well as with the excited $Na^*(^2P_{1/2,3/2})$ atoms. Several processes may contribute to a reduction of the number of fluorescence transitions. Comparing the results for helium and argon gases, we found that the LIF signal decreases faster for helium than for argon. Transients could be taken for helium environments at pressures up to about 400 bar while a signal at 1000 bar for argon gas still could be detected (see Figures 6 and 7, respectively). In

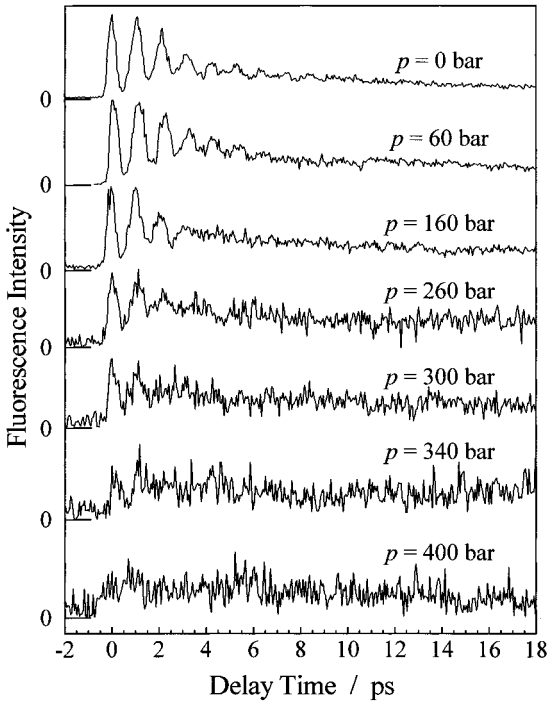

Figure 6. Pump−probe transients taken from NaI in the high-pressure cell for different helium gas pressures. Transients could be taken for helium environments at pressures up to about 400 bar.

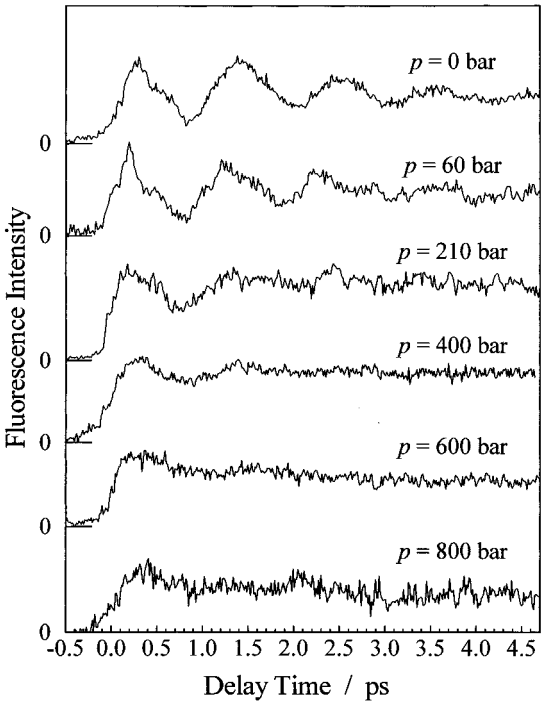

Figure 7. Pump−probe transients taken from NaI in the high-pressure cell for different argon gas pressures. Transients could be taken for argon environments at pressures up to about 1000 bar.

the following we discuss three possibilities: caging, quenching, and vibrational relaxation within the C(0^+) state.

First of all, it seems that the decrease of the LIF intensity depends on the frequency of collisions between the NaI molecules and the surrounding rare-gas atoms. For simplicity, we assume a hard-sphere model, where the collision frequency is given by[20]

$$z_{\mathrm{NaI-RG}} \approx \pi d^2_{\mathrm{NaI-RG}} \left(\frac{8kT}{\pi\mu_{\mathrm{NaI-RG}}}\right)^{1/2} N_{\mathrm{A}}\rho = \sigma_{\mathrm{NaI-RG}}\, \bar{v}\, N_{\mathrm{A}}\rho \tag{4}$$

Here, the collision diameter $d_{\mathrm{NaI-RG}}$ (m) is taken as the mean value of the Lennard-Jones diameters of the rare-gas atom and the NaI molecule, $d_{\mathrm{NaI-RG}} = (d_{\mathrm{LJ}}(\mathrm{NaI}) + d_{\mathrm{LJ}}(\mathrm{RG}))/2$. $\mu_{\mathrm{NaI-RG}}$ is the reduced mass of the collision complex. N_{A} is Avogadro's number and ρ the macroscopic solvent density (mol/L). $\sigma_{\mathrm{NaI-RG}}$ is the cross section (m^2) and $\bar{v}$ the mean thermal velocity (m/s) of the collision pair. In the limit of low-pressure gas $\rho \approx p/RT$. Using this simple model we can approximate the number of collisions as a function of time and pressure of the rare-gas which is shown in Figure 8 for helium and argon gas. The calculated number of collisions per molecule is about 2.3 times higher for helium than for argon.

The cage effect, which means the recombination of the dissociation fragments due to collisions with the surrounding solvent atoms, is more effective for higher masses and larger diameters of the cage atoms.[20] If caging would be the main process responsible for the decrease of fluorescence intensity, one would expect argon to be more efficient.[20] Therefore, caging seems not to be the only process responsible for the decrease in the LIF intensity.

Collisional quenching effects also would result in a decrease of the detected LIF arising from the Na ← Na* transition. If we assume that the quenching rate Q is only a function of the temperature T, the number of moles n_i, the mean velocity $\bar{v}_i$, and the cross section σ_i of the collision partners (e.g. NaI and Ar), the Q is given by[38]

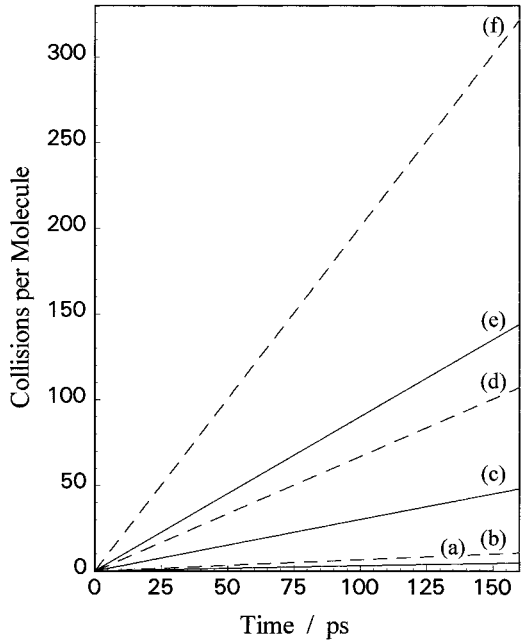

Figure 8. Number of NaI−solution collisions as a function of time and of pressure of rare gas for helium (dashed lines) and argon gas (full lines) calculated using a simple hard-sphere model (eq 4). (a) Ar, $p = 10$ bar; (b) He, $p = 10$ bar; (c) Ar, p 100 bar; (d) He, $p = 100$ bar; (e) Ar, $p = 300$ bar; (f) He, $p = 300$ bar.

$$Q = \sum_i n_i \sigma_i (\bar{v}_i^2)^{1/2} \tag{5}$$

Taking $n_i = p_i/kT$ and $\bar{v}_i^2 = 3kT/m_i$, where p_i is the partial pressure and m_i the mass of the particles, and introducing the total mass $m_{\mathrm{t}} = \sum_i m_i$ and the total pressure $p_{\mathrm{t}} = \sum_i p_i$, the

quenching rate can be written as

$$Q = \sqrt{\frac{3}{m_t kT}}\, p_t \sum_i \sqrt{\frac{m_g}{m_i}}\, \frac{p_i}{p_t}\sigma_i = \sqrt{\frac{3}{m_t kT}}\, p_t \bar{\sigma} \qquad (6)$$

where $\bar{\sigma} := \sum_i (m_g/m_i)^{1/2}(p_i/p)$ is the mean cross section,[38] which is assumed to be independent of the molecular quantum state. From eq 6 we get a quenching rate for argon which is ≈1.4 times higher than that for helium. Similar to the caging, argon gas should result in a more effective reduction of the fluorescence signal by the quenching process than helium gas. This is in agreement with the observations made for iodine. Capelle and Broida[39] measured cross sections for the electronic quenching of iodine of 1.4 and 17.6 Å^2 for helium and argon, respectively.

The C(0^+) state can be described by a shallow Morse potential having a dissociation energy between about 500 and 2000 cm^{-1}.[31,40,41] As the probe pulse prepares the C(0^+) state near its dissociation limit, vibrational relaxation due to collisions with rare-gas atoms might stabilize the NaI molecules below the dissociation limit. Again, argon atoms should result in a larger momentum transfer than helium atoms. If, however, only one collision is sufficient to reduce the energy of NaI below the dissociation energy, then the number of collisions is relevant. In this case, helium would result in a more efficient termination of the fluorescence signal arising from the Na ← Na* transition (compare with results given in Figure 8). At the same time one would expect fluorescence from the C(0^+)) state.[40,41] However, as the stray light from the probe laser has about the same wavelength as the emitted fluorescence, the detection of this emission is rather difficult. Further experiments will be performed to elucidate this topic.

Due to the described experimental problem, it was not possible to observe the influence of caging processes on the first excited state. Other, fluorescence-free probe mechanisms have to be applied in order to receive detailed transients even at high pressures. Experiments making use of nonlinear four-wave-mixing processes[42,43] for probing are in progress.

(ii) The change of the decay behavior of the overall signal intensity also means that the decay of the fluorescence signal can no longer be described by a simple exponential fit. This is shown in Figure 5b,c for helium pressures of $p = 50$ bar and $p = 100$ bar, respectively. Due to the NaI−solvent collisions, the energy of the wave packet propagating within the adiabatic A(0^+) potential well decreases steadily. The vibrational relaxation process is a function of both the rare-gas density and the mass and size of the solvent atoms. Due to the considerable decrease in signal intensity for higher rare-gas pressures, only an estimation can be given for the dependence of vibrational relaxation times on gas densities. It was found that the change of the vibrational relaxation rate is about linearly correlated to the density (pressure) of the rare-gas atoms. This proportionality between rates and density indicates the applicability of isolated binary collision models to the reaction dynamics of the considered system that is reasonable for the pressures used in the experiments. This confirms previous results obtained for iodine in high-pressure rare gases.[20−22] The reaction rate for vibrational relaxation k_{VR} is proportional to the collision frequency z_{NaI-RG}:[44]

$$k_{VR} = P_{VR} \cdot z_{NaI-RG} \qquad (7)$$

P_{VR} gives the probability for reaction per collision and can be expressed by a cross section for vibrational relaxation σ_{VR}:

$$P_{VR} = \frac{\sigma_{VR}}{\sigma_{NaI-RG}} \qquad (8)$$

Using eq 4 in the low-pressure limit then results in:

$$k_{VR} = \sigma_{VR}\bar{v}N_A\rho = \frac{\sigma_{VR}\bar{v}N_A p}{RT} \qquad (9)$$

As $z_{NaI-He} > z_{NaI-Ar}$, our experiments result in $\sigma_{VR}(He) < \sigma_{VR}(Ar)$, which is analogous to the findings from experiments on iodine in high-pressure rare gases.[20−22]

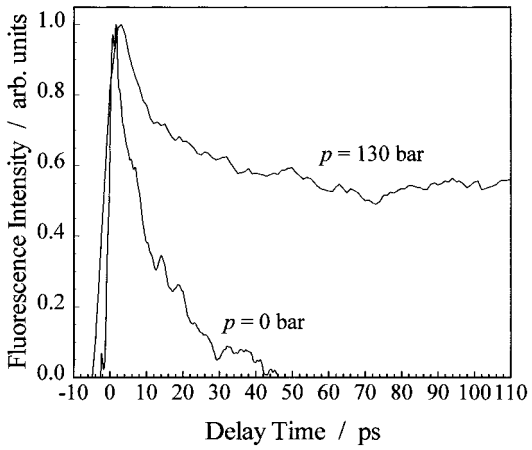

Figure 9. Pump−probe transients taken from NaI in the high-pressure cell for different argon gas pressures. The LIF signal from off-resonance probing at pressures higher than about 50 bar stays at a constant level within the range of accessible delay times (>1 ns).

In the course of vibrational relaxation the total energy E of the wave packet within the adiabatic A(0^+) potential declines. The energy E is an important parameter for the dissociation probability due to the Landau−Zener curve crossing (see eq 2). The probability P_{LZ} decreases with decreasing vibrational energy E_v proportional to $\exp(-a/(E_v)^{1/2})$, where a is a constant.[34] While at $p = 0$ bar the molecules completely dissociate within less than 100 ps, for rising rare-gas pressures a stabilization of the adiabatic state can be found. The LIF signal from off-resonance probing at pressures higher than about 50 bar stays at a constant level within the range of accessible delay times (>1 ns). This behavior is demonstrated in Figure 9 for argon gas pressures of 0 and 130 bar.

For an argon gas pressure of 130 bar the fluorescence signal reaches its constant level after about 50 ps. This corresponds to about 15 NaI−Ar collisions per NaI molecule (see Figure 8). The ratio between signal intensity at $\Delta t = 0$ and the constant signal intensity for long delay times decreases for higher pressures as the vibrational relaxation process becomes faster. Due to the smaller cross section for vibrational relaxation the stabilization process requires higher pressures for helium gas. The possibility that due to pressure-induced potential shifts the probe pulse at $\lambda_{pr} = 620$ nm also probes Na atoms resulting in a constant signal level could be ruled out. No Na atoms could be on-resonantly excited at higher pressures, which points to an efficient caging process.

(iii) From Figures 6 and 7 it is obvious that coherence lifetimes decrease with increasing rare-gas pressure. We have monitored the coherent wave packet motion in the A(0^+) state over tens of picoseconds. In an isolated NaI molecule, the femtosecond excitation creates a coherent vibrational wave packet.[45] Due to the anharmonicity of the potential, dephasing and rephasing processes occur, resulting in a modulation of the

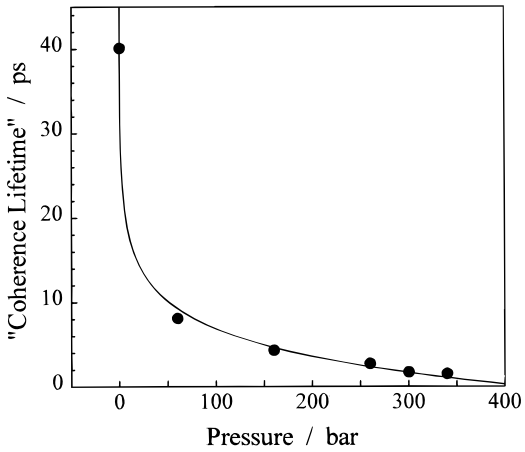

Figure 10. Pressure dependence of the "coherence lifetime" τ_{coh} of the wave packet within the adiabatic $A(0^+)$ potential well of NaI as a function of helium gas pressure.

oscillation amplitudes of the transient signal. For $p = 0$ bar, at about 30−40 ps delay time weak revivals can be found for NaI, which is consistent with the findings of Cong *et al.*[46] Therefore, the coherence lifetime can be estimated to be longer than 40 ps for free NaI molecules.[45] However, even very low pressures of rare gas have a considerable effect on the phase of the wave packet motion. The amplitudes of the oscillations decrease very fast, and no more rephasing can be found. Assuming the last observed oscillation as a crude measure for the coherence lifetime τ_{coh}, we find an exponential decay of τ_{coh} with pressure. This is shown in Figure 10 for helium gas. As for low pressures on the short time intervals considered only few NaI−solution collisions take place, single binary collisions are not only responsible for vibrational relaxation but also for fast dephasing of the wave packets.

For a quantitative evaluation one further observation has to be taken into account. In the transients taken from NaI in argon gas a pulse broadening for increasing pressures is indicated by the changing rise of the signal near time zero (see e.g. Figure 7). Such a broadening is not observed for helium gas, which is due to its much smaller polarizability. The broadening of the pulses also might influence the vibrational coherence loss. However, comparable experiments performed on iodine in rare-gas environments point to a negligible influence of the broadening effect in argon on the molecular dynamics.[20−22] As the broadening is power dependent, experiments using different laser powers would help to investigate this effect in more detail. Recently, it was shown that NaI transients are highly dependent on the laser intensity if the probe laser is resonant with the Na ← Na* transition (on-resonant).[30] However, the shape of the transients probing the transition state (off-resonant) is not influenced by the change of laser power. Therefore, broadening effects could be directly seen from the changes in the transient shape. Due to the difficulties detecting the LIF signal at higher rare-gas pressures (see discussion above), a fluorescence free probe technique has to be applied. Experiments using nonlinear four-wave mixing[43] are in progress.

For a detailed analysis of the experimental results, a reproduction of the data by means of quantum mechanical molecular dynamics simulations is in progress and will be published in due time.[47]

4. Conclusions

In this study, we have employed femtosecond transition-state spectroscopy to explore the influence of rare-gas collisions on coherent wave packet motion in NaI. The experiments were performed in compressed supercritical argon or helium gas at a temperature of 670 °C and pressure ranging from 0 to 1000 bar. Ground-state NaI molecules were excited with femtosecond pump pulses (320 nm) resulting in a vertical transition from the ionic to the covalent potential curves [$A(0^+,1) \leftarrow X(^1\Sigma^+)$]. By choosing an appropriate wavelength for the femtosecond probe pulse (620 nm), the wave packet dynamics belonging to the $[Na\cdots I]^{\ddagger *}$ transition state could be followed as a function of delay time between pump and probe pulses.

For free NaI molecules the well-known wave packet dynamics within the adiabatic potential well formed by the interaction of ground $X(^1\Sigma^+)$ and excited $A(0^+)$ states could be seen. The transient displayed the oscillatory behavior of the wave packet within the adiabatic $A(0^+)$ potential. A Fourier transform calculation resulted in a dominant contribution corresponding to a wavenumber difference of 27.5 cm^{-1} between adjacent vibrational eigenstates. The decay of the signal intensity due to the population loss by predissociation, caused by the non-Born−Oppenheimer coupling of the ionic and covalent states, could be simulated using the Landau−Zener model for the avoided crossing. The Landau−Zener escape probability was found to be $P_{LZ} \approx 0.10$. The oscillation amplitudes of the transient signals were modulated due to dephasing and rephasing processes, caused by the anharmonicity of the potential. Revivals could be detected at about 30−40 ps. These observations are consistent with earlier findings (see e.g. ref 45).

Upon going to higher rare-gas pressures, several changes could be observed. Due to collisions with the rare-gas atoms, the intensity of the detected laser-induced fluorescence, arising from the Na ← Na* transition, decreases considerably. Only transients up to 1000 bar for argon gas and 400 bar for helium gas could be obtained. A simple hard-sphere model gave ca. 2.3 times higher collision frequencies for helium than for argon. However, the efficiency for caging or quenching processes is expected to be higher for argon than for helium atoms as it was observed for similar interactions between iodine molecules and rare-gas atoms.[20−22,39] Therefore, the contribution of a process scaling with the collision rate had to be considered. As a possible explanation a stabilization of the excited NaI molecules below the dissociation limit of the $C(0^+)$ state is discussed.

For the influence of the rare-gas collisions on the transition state dynamics of NaI a reversed behavior could be found. Here, helium gas interacts with a smaller reaction cross section than argon gas similar to the findings made for iodine.

Even for low rare-gas pressures a considerable change of the coherent wave packet motion within the adiabatic $A(0^+)$ potential well could be found. Only few NaI−solution collisions resulted in fast vibrational relaxation. Due to the energy loss, the Landau−Zener escape probability decreases in the course of the relaxation process. This results in a stabilization of the transition state for higher pressures. In the experiments this reflects long living (>1 ns) constant transient signals. For helium and argon gas the collision-induced vibrational relaxation leading to the stabilized state increased nearly linearly with density (pressure). This indicates the applicability of isolated binary collision models to the reaction dynamics influenced by high-pressure gases, which is a reasonable assumption for the pressures applied. However, the coherence lifetime of the wave packet was found to decrease exponentially with rare-gas pressure. No more coherent wave packet motion could be detected for rare-gas pressures higher than 400 bar.

A possible influence of pulse broadening in argon gas on the observed coherence lifetime is discussed. In order to clarify this issue, further experiments have to be done.

Due to the quenching of the probe laser-induced fluorescence

signal, the signal-to-noise ratio was pure for higher pressures. Therefore, we were not able to observe possible caging processes that might occur at higher pressures. Additionally, a quantitative analysis of the experimental data is very difficult. Therefore, in future experiments different probe techniques have to be applied, as, for example, nonlinear four-wave-mixing processes. In order to gain a better understanding of the experimental results, quantum mechanical molecular dynamics simulations are in progress.[47]

Acknowledgment. This article is dedicated to Professor Ahmed H. Zewail. His pioneering work established femtochemistry as new research area in science and inspires an increasing number of researchers. One of us (A.M.) is especially thankful for the valuable experiences gathered in Professor Zewail's group as a postdoctoral fellow. This work was funded by the Deutsche Forschungsgemeinschaft (Schwerpunktprojekt MA 1564/3-1). Stimulating discussions with Holger Dietz and Professor Volker Engel are gratefully acknowledged.

References and Notes

(1) Hynes, T. *Annu. Rev. Phys. Chem.* **1985**, *36*, 573.
(2) Ulstrop, J. In *Charge Transfer Processes in Condensed Media*; Springer: New York, 1979.
(3) Franck, J.; Rabinowitch, E. *Trans. Faraday. Soc.* **1930**, *30*, 120.
(4) Rabinowitch, E.; Wood, W. C. *Trans. Faraday. Soc.* **1936**, *32*, 547.
(5) Zimmerman, J.; Noyes, R. M. *J. Chem. Phys.* **1950**, *18*, 658.
(6) Harris, A. L.; Brown, J. K.; Harris, C. B. *Annu. Rev. Phys. Chem.* **1988**, *39*, 341.
(7) Chuang, T. J.; Hoffmann, G. W.; Eisenthal, K. B. *Chem. Phys. Lett.* **1974**, *25*, 201.
(8) Nesbitt, D.; Hynes, J. T. *J. Chem. Phys.* **1982**, *77*, 2130.
(9) Bado, P.; Berens, P. H.; Wilson, K. R. *Proc. Soc. Photo-Opt. Instrum. Eng.* **1982**, *332*, 230.
(10) Kelley, D. F.; Abul-Haj, N. A.; Jang, D. J. *J. Chem. Phys.* **1984**, *80*, 4105.
(11) Berg, M.; Harris, A. L.; Harris, C. B. *Phys. Rev. Lett.* **1985**, *54*, 951.
(12) Paige, M. E.; Harris, C. B. *Chem. Phys.* **1990**, *149*, 37.
(13) Bowman, R. M.; Dantus, M.; Zewail, A. H. *Chem. Phys. Lett.* **1989**, *161*, 297.
(14) Dantus, M.; Janssen, M. H. M.; Zewail, A. H. *Chem. Phys. Lett.* **1991**, *181*, 281.
(15) Yan, Y.; Whitnell, R. M.; Wilson, K. R.; Zewail, A. H. *Chem. Phys. Lett.* **1992**, *193*, 402.
(16) Zewail, A. H.; Dantus, M.; Bowman, R. M.; Mokhtari, A. *J. Photochem. Photobiol. A* **1992**, *62*, 301.
(17) Breen, J. J.; Willberg, D. M.; Zewail, A. H. *J. Chem. Phys.* **1990**, *93*, 9180.
(18) Willberg, D. M.; Gutmann, M.; Breen, J. J.; Zewail, A. H. *J. Chem. Phys.* **1992**, *96*, 198.
(19) Zewail, A. H. *Femtochemistry: Ultrafast Dynamics of the Chemical Bond*; World Scientific: Singapore, 1994.
(20) Lienau, C.; Zewail, A. H. *J. Phys. Chem.* **1996**, *100*, 18629.
(21) Materny, A.; Lienau, C.; Zewail, A. H. *J. Phys. Chem.* **1996**, *100*, 18650.
(22) Liu, Q.; Wan, C.; Zewail, A. H. *J. Phys. Chem.* **1996**, *100*, 18666.
(23) Scherer, N. F.; Ziegler, L. D.; Fleming, G. R. *J. Chem. Phys.* **1992**, *96*, 5544.
(24) Wang, J. K.; Liu, Q.; Zewail, A. H. *J. Phys. Chem.* **1995**, *99*, 11309.
(25) Zadoyan, R.; Li, Z.; Martens, C. C.; Apkarian, V. A. *J. Chem. Phys.* **1994**, *101*, 6648.
(26) Li, Z.; Zadoyan, R.; Apkarian, V. A.; Martens, C. C. *J. Phys. Chem.* **1995**, *99*, 7453.
(27) Rose, T. S.; Rosker, M. J.; Zewail, A. H. *J. Chem. Phys.* **1988**, *88*, 6672.
(28) Rosker, M. J.; Rose, T. S.; Zewail, A. H. *Chem. Phys. Lett.* **1988**, *146*, 175.
(29) Rose, T. S.; Rosker, M. J.; Zewail, A. H. *J. Chem. Phys.* **1989**, *91*, 7415.
(30) Materny, A.; Herek, J. L.; Cong, P.; Zewail, A. H. *J. Phys. Chem.* **1994**, *98*, 3352.
(31) Cong, P.; Roberts, G.; Herek, J. L.; Mohktari, A.; Zewail, A. H. *J. Phys. Chem.* **1996**, *100*, 7832.
(32) Engel, V.; Metiu, H.; Ameida, R.; Marcus, R. A.; Zewail, A. H. *Chem. Phys. Lett.* **1988**, *152*, 1. Engel, V.; Metiu, H. *J. Chem. Phys.* **1989**, *90*, 6116.
(33) Schäfer, S. H.; Bender, D.; Tiemann, E. *Chem. Phys.* **1984**, *89*, 65.
(34) Bersohn, R.; Zewail, A. H. *Ber. Bunsen-Ges. Phys. Chem.* **1988**, *92*, 373.
(35) Bernstein, R. B.; Zewail, A. H. *J. Chem. Phys.* **1989**, *90*, 829.
(36) Landau, L. *Phys. Z. Sowjetunion* **1932**, *2*, 46. Zener, C. *Proc. R. Soc. London A* **1933**, *137*, 696. *Ibid.* **1933**, *140*, 660. Levine, R. D.; Bernstein, R. B. *Molecular Reaction Dynamics and Chemical Reactivity*; Oxford University Press: New York, 1987.
(37) White, J. C. *Appl. Phys. Lett.* **1979**, *33*, 335.
(38) Garland, N. L.; Crosley, D. R. *Symp. Combust. 21st* **1986**, *39*, 1693.
(39) Capelle, G. A.; Broida, H. P. *J. Chem. Phys.* **1973**, *58*, 4212.
(40) Bower, R. D.; Chevrier, P.; Das, P.; Foth, H. J.; Polanyi, J. C.; Prisant, M. G.; Visticot, J. *J. Chem. Phys.* **1988**, *89*, 4478.
(41) Bluhm, H.; Lindner, J.; Tiemann, E. J. *J. Chem. Phys.* **1990**, *93*, 4556.
(42) Motzkus, M.; Pedersen, S.; Zewail, A. H. *J. Phys. Chem.* **1996**, *100*, 5620.
(43) Schmitt, M.; Knopp, G.; Materny, A.; Kiefer, W. *Chem. Phys. Lett.* **1997**, *270*, 9.
(44) Chesnoy, J.; Weis, J. J. *J. Chem. Phys.* **1986**, *84*, 5378.
(45) Zewail, A. H. *Faraday Discuss. Chem. Soc.* **1991**, *91*, 207.
(46) Cong, P.; Mokhtari, A.; Zewail, A. H. *Chem. Phys. Lett.* **1990**, *172*, 109.
(47) Dietz, H.; Knopp, G.; Materny, A.; Engel, V. To be published.